



OIST

OKINAWA INSTITUTE OF SCIENCE AND TECHNOLOGY GRADUATE UNIVERSITY  
沖縄科学技術大学院大学

## Dynamic stereoselective annulation via aldol-oxa-cyclization cascade reaction to afford spirooxindole pyran polycycles

|                              |   |
|------------------------------|---|
| Author                       | Muhammad Sohail, Fujie Tanaka   |
| journal or publication title | Communications Chemistry  |
| volume                       | 2   |
| number                       | 1   |
| page range                   | 73  |
| year                         | 2019-06-28  |
| Publisher                    | Nature Research   |
| Rights                       | (C) 2019 The Author(s).   |
| Author's flag                | publisher   |
| URL                          | <a href="http://id.nii.ac.jp/1394/00001071/">http://id.nii.ac.jp/1394/00001071/</a> |

doi: info:doi/10.1038/s42004-019-0177-5

ARTICLE

<https://doi.org/10.1038/s42004-019-0177-5>

OPEN

# Dynamic stereoselective annulation via aldol-oxa-cyclization cascade reaction to afford spirooxindole pyran polycycles

Muhammad Sohail <sup>1</sup> & Fujie Tanaka <sup>1</sup>

Spiro polycyclic compounds bearing pyran ring systems are found in bioactive molecules, and we recently reported the construction of spirooxindole all-carbon polycycles. Here we show the development of catalytic stereoselective annulation reactions that afford spirooxindole pyran polycycles. Oxindole-derived spiro[4,5]decanes are reacted with arylglyoxal to construct a pyran ring via the formation of carbon-carbon and carbon-oxygen bonds through dynamic aldol-oxa-cyclization cascade reactions, leading to the formation of spirooxindole pyran polycycles bearing six stereogenic centers as single diastereomers. During the reaction, the starting material is isomerized to the diastereomer, and this is key to afford the product. Taking advantage of this isomerization, highly enantiomerically enriched single diastereomers of spirooxindole pyran polycycles are obtained. The reactions generating the spiro pyran polycycles show stereoselectivities distinct from those previously observed in the construction of all-carbon polycycles.

<sup>1</sup>Chemistry and Chemical Bioengineering Unit, Okinawa Institute of Science and Technology Graduate University, 1919-1 Tancha, Onna, Okinawa 904-0495, Japan. Correspondence and requests for materials should be addressed to F.T. (email: [ftanaka@oist.jp](mailto:ftanaka@oist.jp))

Pyran-derived polycycles bearing spiro ring systems and spirooxindole scaffolds are found in bioactive natural products and pharmaceutical agents<sup>1–6</sup> (Fig. 1a). Whereas syntheses of many classes of spirooxindole polycycles bearing N-heterocycles and spirooxindole all-carbon polycycles have been reported<sup>7–21</sup>, few examples of the syntheses of spirooxindole polycycles bearing O-heterocycles have been reported<sup>22,23</sup>. Most methods developed for the synthesis of the spirooxindole O-heterocycles provide nonpolycyclic derivatives<sup>24–33</sup>. Because the lengths of C–C, C–N, and C–O bonds are different, spirooxindole polycyclic scaffolds bearing oxygen-containing heterocycles should provide molecules with biological functions different from those of spirooxindole all-carbon polycyclic and N-heterocycle-containing polycyclic systems.

In addition, the construction of polycyclic molecules through the formation of C–C and C–O bonds would provide structures with unique regio- and diastereoselectivities compared to those accessed via the formation of C–C and C–N bonds. Thus, the development of strategies and methods that provide access to polycyclic scaffolds<sup>21,34–37</sup> bearing O-heterocycles and spirooxindole cores is of interest in drug discovery efforts and related research.

Here, we report a route to functionalized spirooxindole pyran polycycles. We report stereoselective construction of pyran polycycles using annulation reactions via the formation of C–C and C–O bonds; these reactions provide products with stereoselectivities distinct from those demonstrated in the formation of all-carbon polycycles (Fig. 1b, c).

## Results

**Design.** Our strategy for the construction of spirooxindole pyran polycycles uses oxindole-derived spiro[4,5]decanes<sup>21</sup> as starting

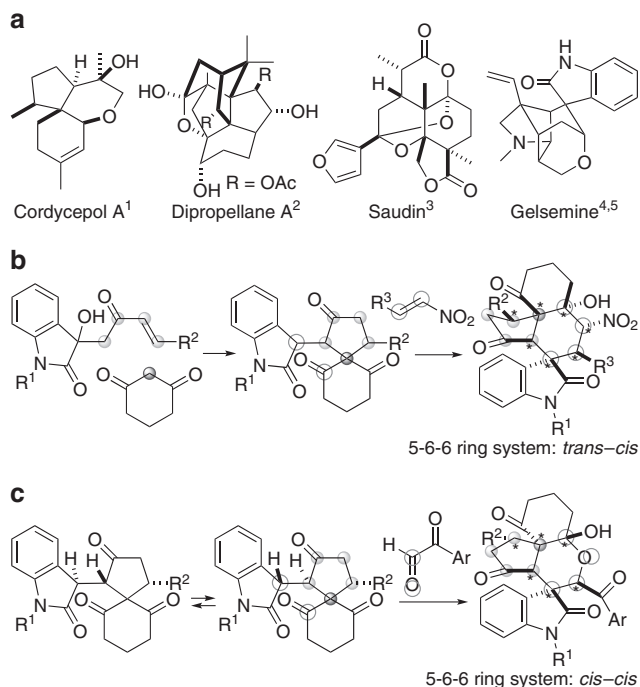


**Fig. 1** Development of reactions to afford spirooxindole pyran polycycles. **a** Bioactive pyran polycycles<sup>1–5</sup>. **b** Synthesis of spirooxindole all-carbon polycycles from spiro[4,5]decane derivatives<sup>21</sup>. **c** Synthesis of spirooxindole pyran polycycles from the same spiro[4,5]decane derivatives (this study). The dynamic aldol-oxa-cyclization cascade reactions (reactions with C=O, in **c**) that provide pyran polycycles described here show stereoselectivities distinct from those previously observed in the Michael–Henry cascade reactions (reactions with C=C, in **b**)

materials (Fig. 1c). We have recently reported the construction of spirooxindole all-carbon polycyclic systems from one of the diastereomers of the spiro[4,5]decanes by the reactions with nitrostyrenes<sup>21</sup> (Fig. 1b). Here, we used the same starting molecules, spiro[4,5]decanes and their diastereomers, and reacted these with arylglyoxals through aldol-oxa-cyclization cascade reactions to construct a pyran ring, leading to the formation of the spirooxindole pyran polycycles. We hypothesized that the actual reacting diastereomers of the spiro[4,5]decanes and the bond-forming positions would depend on reaction partners and the type of the bond formed (i.e., C–C or C–O). We also hypothesized that stereoselective formation of products would be achieved by selecting suitable catalysts and conditions including those that are involved in isomerization and equilibration of the reactants and the intermediates<sup>36,38–40</sup>.

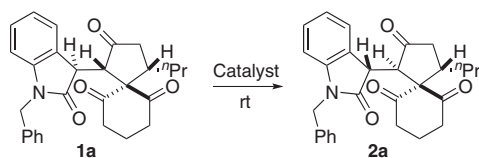
## Conditions for the formation of the spirooxindole pyran polycycles.

First, catalysts and conditions were evaluated to identify those that catalyzed the reactions of oxindole-derived spiro[4,5]decane **1a** or its diastereomer **2a** with phenylglyoxal to afford pyran-derived polycycles (Table 1). Using DABCO as catalyst at room temperature (rt, 25 °C) in CH<sub>2</sub>Cl<sub>2</sub>, spirooxindole pyran polycycle **3a** was formed from **2a** (Table 1, entry 2). However, under the same conditions with **1a** instead of **2a**, formation of **3a** was not detected (Table 1, entry 1). The use of DBU instead of DABCO under otherwise the same conditions led to the formation of **3a** from **1a** (Table 1, entry 3). With the use of DBU as catalyst under appropriate conditions, product **3a** was obtained from both the reactions of **1a** and of **2a** (Table 1, entries 4 and 5). Relative stereochemistry of **3a** was determined by X-ray crystal structural analysis, and the result indicated that **3a** was derived from **2a** (i.e., **3a** retained the stereochemistries of the stereogenic centers in the cyclopentane ring of **2a**). No formation of other diastereomers and of other products was observed under the conditions listed in Table 1. These results suggested that, with **1a** as starting material, **1a** first isomerized to **2a**, and **2a** reacted with phenylglyoxal to give **3a**. When the reaction was performed in the presence of DBU (0.2 equiv) as catalyst with addition of

**Table 1** Formation of **3a** from **1a** and from **2a**<sup>a</sup>

| Entry            | sm        | Catalyst (equiv) | Solvent                         | Temperature | <b>3a</b> yield (%) <sup>b</sup> |
|------------------|-----------|------------------|---------------------------------|-------------|----------------------------------|
| 1                | <b>1a</b> | DABCO (0.2)      | CH <sub>2</sub> Cl <sub>2</sub> | rt (25 °C)  | 0                                |
| 2                | <b>2a</b> | DABCO (0.2)      | CH <sub>2</sub> Cl <sub>2</sub> | rt (25 °C)  | 27                               |
| 3                | <b>1a</b> | DBU (0.2)        | CH <sub>2</sub> Cl <sub>2</sub> | rt (25 °C)  | 19                               |
| 4 <sup>c</sup>   | <b>1a</b> | DBU (0.2)        | CHCl <sub>3</sub>               | 0 °C        | 64                               |
| 5 <sup>c</sup>   | <b>2a</b> | DBU (0.2)        | CHCl <sub>3</sub>               | 0 °C        | 63                               |
| 6 <sup>c,d</sup> | <b>1a</b> | DBU (0.2)        | CHCl <sub>3</sub>               | 0 °C        | 91 (90) <sup>e</sup>             |
| 7 <sup>c,d</sup> | <b>2a</b> | DBU (0.2)        | CHCl <sub>3</sub>               | 0 °C        | 90                               |
| 8 <sup>c,d</sup> | <b>1a</b> | DBU (0.1)        | CHCl <sub>3</sub>               | 0 °C        | 83                               |
| 9 <sup>c,d</sup> | <b>1a</b> | DBU (0.05)       | CHCl <sub>3</sub>               | 0 °C        | 40                               |

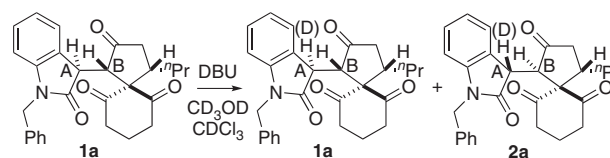
<sup>a</sup>Conditions: Starting material (sm) **1a** or **2a** (0.03 mmol, 1.0 equiv), phenylglyoxal monohydrate (1.5 equiv), and catalyst in solvent (0.5 mL) for 12 h. DABCO = 1,4-diazabicyclo[2.2.2]octane. DBU = 1,8-diazabicyclo[5.4.0]undec-7-ene.  
<sup>b</sup>Determined by <sup>1</sup>H NMR analysis of the reaction mixture.  
<sup>c</sup>Solvent (0.1 mL).  
<sup>d</sup>H<sub>2</sub>O (1.0 equiv) was added and phenylglyoxal monohydrate (4.5 equiv) was used.  
<sup>e</sup>Isolated yield.

**Table 2 Catalysts and conditions for the isomerization of 1a to 2a<sup>a</sup>**

| Entry          | Catalyst (equiv)                     | Time  | Ratio 1a:2a |
|----------------|--------------------------------------|-------|-------------|
| 1              | Pyridine (0.1)                       | 72 h  | 100:0       |
| 2              | Et <sub>3</sub> N (0.1)              | 10 h  | 97:3        |
| 3              | DABCO (0.1)                          | 10 h  | 90:10       |
| 4              | DBU (0.1)                            | 5 min | 29:71       |
| 5              | DBU (0.1)                            | 10 h  | 29:71       |
| 6              | DBU-CH <sub>3</sub> COOH (1:1) (0.1) | 10 h  | 100:0       |
| 7              | DBU (0.01)                           | 5 min | 25:75       |
| 8              | DBU (0.001)                          | 5 min | 22:78       |
| 9 <sup>b</sup> | DBU (0.001)                          | 5 min | 22:78       |

<sup>a</sup>Conditions: **1a** (0.03 mmol, 1.0 equiv) and catalyst in CHCl<sub>3</sub> (1.0 mL) at rt (25 °C) except where noted

<sup>b</sup>**2a** was used instead of **1a**

**Table 3 Deuteration during the isomerization of 1a: proton integration at positions A and B of 1a and of 2a under the DBU-catalyzed isomerization<sup>a</sup>**

| Entry          | Time (min) | 1a, A | 1a, B | 2a, A | 2a, B | 1a:2a |
|----------------|------------|-------|-------|-------|-------|-------|
| 1 <sup>b</sup> | —          | 1.0   | 1.0   | —     | —     | 98:2  |
| 2 <sup>c</sup> | —          | 1.0   | 1.0   | —     | —     | 98:2  |
| 3              | 1          | 0.2   | 1.0   | 0.4   | 1.0   | 40:60 |
| 4              | 6          | 0.2   | 1.0   | 0.3   | 1.0   | 37:63 |
| 5              | 10         | 0.1   | 1.0   | 0.3   | 1.0   | 37:63 |
| 6              | 15         | 0.1   | 1.0   | 0.2   | 1.0   | 35:65 |
| 7              | 20         | 0.1   | 1.0   | 0.2   | 1.0   | 34:66 |
| 8              | 472        | 0.1   | 1.0   | 0.2   | 1.0   | 29:71 |

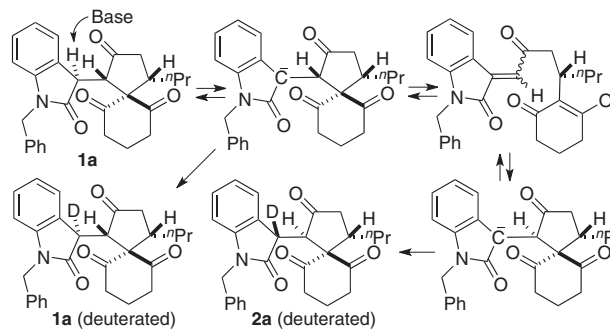
<sup>a</sup>Integration of H at the indicated position relative to the integration of a proton at the benzylic position of the benzyl group of the respective compound is listed. 0 min = addition of DBU

<sup>b</sup>Data of **1a** in CDCl<sub>3</sub> before addition of CD<sub>3</sub>OD and DBU

<sup>c</sup>Data of **1a** immediately after addition of CD<sub>3</sub>OD in CDCl<sub>3</sub>

H<sub>2</sub>O as an additive in CHCl<sub>3</sub> at 0 °C, **3a** was obtained in high yields (Table 1, entries 6 and 7). Note that in our previously reported synthesis of spirooxindole all-carbon polycycles, only **1a** reacted with nitrostyrenes to afford the product<sup>21</sup>. The reactions with phenylglyoxal (in which the reactions are with the C=O group) showed distinct stereoselectivities from those previously observed in the construction of the all-carbon cyclohexane ring.

**Isomerization of the starting material.** Because the isomerization from **1a** to **2a** was essential to afford **3a** from **1a**, conditions for the isomerization were evaluated (Table 2). Pyridine did not isomerize **1a** (Table 2, entry 1). Et<sub>3</sub>N and DABCO isomerized **1a** to **2a**, respectively, but the formation of **2a** was slow (Table 2, entries 2 and 3). DBU efficiently isomerized **1a** to **2a**. During the isomerization of **1a**, only the formation of **2a** was observed; no isomers other than **1a** and **2a** were detected. Under the same DBU catalysis conditions, **2a** was also isomerized to **1a** and the ratio between **1a** and **2a** was the same as observed in the isomerization of **1a** (Table 2, entries 8 and 9). These results indicate that the isomerization reactions between **1a** and **2a** reached the equilibrium in the presence of DBU regardless of whether the starting material was **1a** or **2a**. The isomerization between **1a** and **2a** occurred even in the presence of only 0.001 equiv (or 0.1 mol %) loading of DBU (Table 2, entries 8 and 9). To understand the mechanisms of the isomerization of **1a** to **2a**, deuteration experiments were performed under the DBU-catalyzed isomerization conditions (Table 3). To generate **2a** from **1a**, both the stereochemistries at position A (the α-position of the oxindole amide group) and at position B (the α-position of the ketone carbonyl group of the 5-membered ring) of **1a** must be altered. Whereas the proton at position A of **1a** was exchanged with deuterium, the proton at position B of **1a** was not. In the formed **2a**, similarly, position A was deuterated and position B retained H. These results suggest that the isomerization occurs through the enolization of the cyclohexane-1,3-dione moiety with the C–C bond cleaving and forming (Fig. 2). The isomerization and the deuteration results suggest that when compound **1a** is enantiomerically enriched, the enantiomeric ratio (er) of **1a** is retained in **2a**; the stereochemistry of the β-position of the ketone carbonyl group of the cyclopentane ring is not affected by the

**Fig. 2** Proposed mechanisms of the isomerization and the deuteration of **1a** and **2a**. See Tables 2 and 3

isomerization. In fact, when enantiomerically enriched **1a** (er 99.8:0.2) was treated with DBU, **2a** was obtained in essentially the same er (er 99.7:0.3).

**Scope of the annulation reaction.** With the use of enantiomerically enriched **1** as the starting material in the reactions with arylglyoxals, under the conditions optimized for the formation of **3a** from **1a**, various enantiomerically enriched functionalized spirooxindole pyran polycycles **3** were obtained in one pot (Fig. 3). In all the cases, products **3** were isolated as single diastereomers in high yields with high enantiomeric ratios (up to er > 99.9:0.1). Whereas isomerization of **1a** to **2a** occurred in the presence of only 0.001 equiv of DBU as described above, the use of 0.2 equiv of DBU provided better results than the use of low loadings of DBU for the formation of **3**. Hydrated arylglyoxal may act as weak acid to neutralize DBU, resulting in the requirement of the conditions containing 0.2 equiv of DBU for the efficient formation of **3**. The utility of the reactions to form **3** was further demonstrated by the transformations of **3a** to various polycyclic derivatives **4–8** (Fig. 4). Reduction of **3a** using H<sub>2</sub> and Pd/C afforded **4**, in which the ring system was reorganized to provide a new spirooxindole pyran polycycle system. On the other hand, reduction of **3a** using NaBH(OAc)<sub>3</sub> afforded alcohol

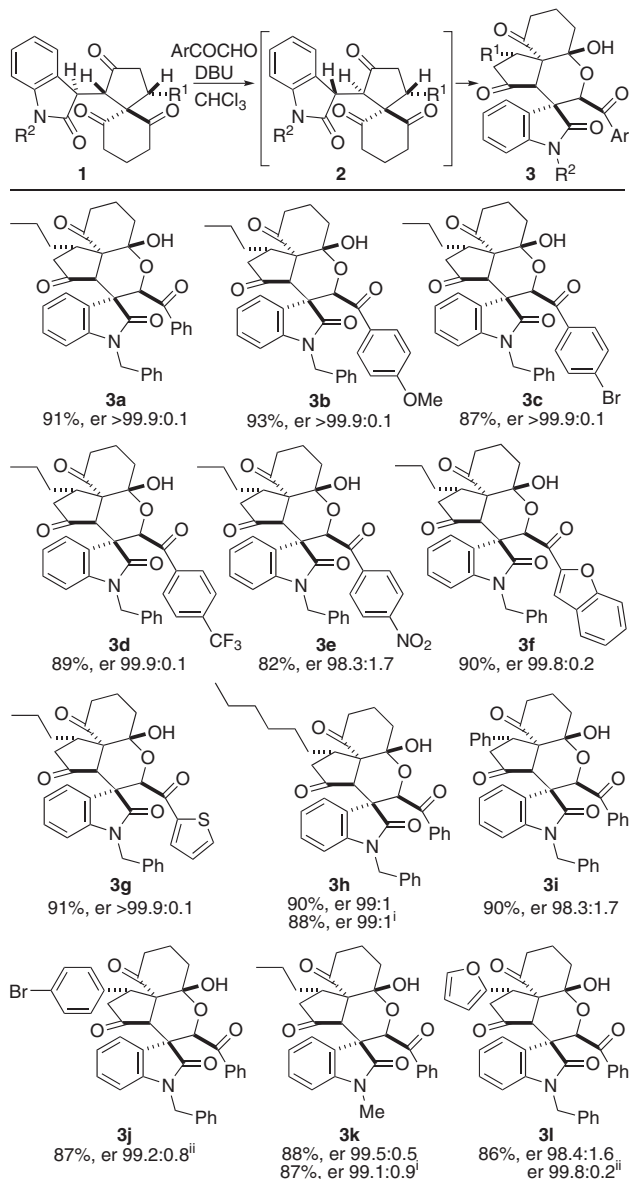


**Fig. 3** Scope of the formation of **3** from **1**. Conditions: **1** (0.23 mmol, 1.0 equiv), DBU (0.2 equiv), H<sub>2</sub>O (1.0 equiv), and arylglyoxal monohydrate (4.5 equiv) in CHCl<sub>3</sub> (0.8 mL), 0 °C, 12 h. (i) **2** was used instead of **1**. (ii) Data after removal of precipitates

**6** without affecting the spiropolycyclic framework. Complex polycycles **7** and halogenated polycyclic products **5** and **8** were also obtained concisely.

**Plausible pathway of the reaction.** Based on the stereochemistry of product **3a**, the reaction pathway for the formation of **3a** from **1a** is suggested as follows: when the cyclopentanone moiety of **1a** had the (*S,S*) configuration, the *si*-face of the  $\alpha$ -position of the oxindole amide group of **2a** reacted with the *re*-face of the aldehyde group of phenylglyoxal during the C–C bond formation (Fig. 5). Then, the oxygen atom that originated from the aldehyde group reacted with the *si*-face of a specific ketone carbonyl group to afford **3a** (Fig. 5a). In the reaction of a single enantiomer of **1a** or **2a** with phenylglyoxal, the number of possible product stereoisomers that may form is 48, calculated from 2 (selection of **1a** or **2a**)  $\times$  2 (reaction face selectivity of **1a** or **2a**)  $\times$  2 (reaction face selectivity of phenylglyoxal)  $\times$  6 (ketone positions and reaction

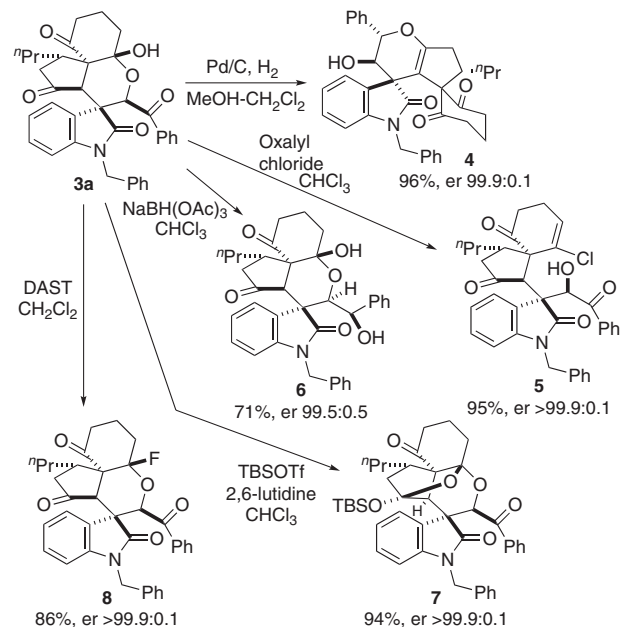


**Fig. 4** Transformations of **3a**. Full details are provided in the Supplementary Methods

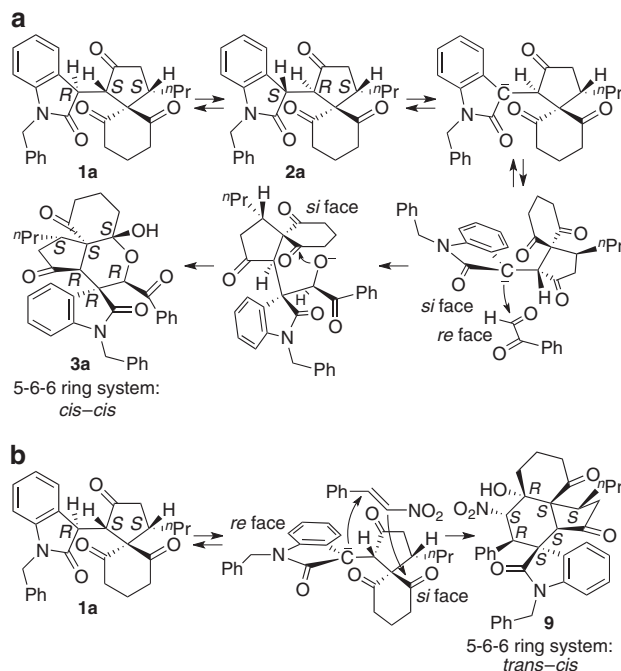


**Fig. 5** Pathways of the reaction. **a** A plausible pathway for the formation of **3a** from **1a**. **b** A plausible pathway for the formation of **9** from **1a** (the formation of **9** was described in ref. 21)

faces of the ketones). During the reaction, formation of product diastereomers other than **3a** and accumulation of intermediates (products of aldol reaction without C–O bond formation) were not detected. These results suggest that reversible processes are involved in the isomerization between **1a** and **2a** and in the aldol reaction C–C bond formation. The results also suggest that the kinetic control in the aldol reaction step is key for the selective formation of **3a**. That is, the aldol C–C bond formation of either **1a** or **2a** with phenylglyoxal may occur without reaction



selectivities, but the aldol adducts that do not lead to the C–O bond formation may be quickly decomposed to the starting materials. The kinetically favoured transition state for the C–C bond formation would determine the reacting ketone group and its face used for the C–O bond formation in the cascade sequence, although the details of the reaction mechanisms will need to be studied further. In the previously reported reaction of **1a** with nitrostyrene<sup>21</sup>, when the cyclopentanone moiety of **1a** had the (S, S) configuration, it is deduced that the *re*-face of **1a** reacted for the C–C bond formation (Fig. 5b) based on the stereochemistry of the product. It is also deduced that the  $\alpha$ -position of the nitro group then reacted with the *si*-face of the specific ketone carbonyl group for the selective formation of product **9**<sup>21</sup>. Product **9** had a *trans*–*cis* relationship for the generated 5–6–6 ring system. In contrast, in the formation of **3a**, the actual reactant was **2a**, and the formed 5–6–6 ring system had a *cis*–*cis* relationship. The annulation via the aldol-oxa-cyclization of **1a** with arylglyoxal showed completely different stereoselectivities from the annulation via the Michael–Henry reaction of **1a** with nitrostyrene.

## Discussion

We have developed catalytic stereoselective annulation reactions that afford spirooxindole pyran polycycles. We have shown that the formation of the pyran ring through the formation of C–C and C–O bonds that result in the formation of the polycyclic system provides stereoselectivities distinct from the formation of the cyclohexane ring through the formation of C–C bonds that lead to the all-carbon polycycles from the same spiro[4,5]decane derivatives. The differences in the reaction stereoselectivities may originate from the differences in C–C and C–O bond lengths. The details of the mechanisms of the reactions that lead to the selective formation of the complex polycyclic products and of the differences in the stereoselectivities between the formation of the pyran polycycles and the formation of previously reported all-carbon polycycles are under investigation. The method reported here provides a way to access spirooxindole pyran polycycles useful for the development of bioactive molecules and related research.

## Methods

**Synthetic procedures.** See Supplementary Methods.

**Isomerization experiments.** See Supplementary Tables 1–5 and Supplementary Figures 1–9.

**Characterization.** For NMR spectra and HPLC chromatograms see Supplementary Figures 10–136.

**Crystallography.** X-ray crystallographic data of compounds ( $\pm$ )-**3a** and ( $\pm$ )-**4a** are available in Supplementary Data 1–2.

## Data availability

X-ray crystallographic data of compounds ( $\pm$ )-**3a** and ( $\pm$ )-**4a** have been deposited at the Cambridge Crystallographic Data Centre (CCDC); compound ( $\pm$ )-**3a** (CCDC 1906368) and compound ( $\pm$ )-**4a** (CCDC 1906367). These data can be obtained free of charge from the CCDC via [www.ccdc.cam.ac.uk/data\\_request/cif](http://www.ccdc.cam.ac.uk/data_request/cif). All other data in support of the findings of this study are available within the article and its Supplementary Information or from the corresponding author upon reasonable request.

Received: 23 April 2019 Accepted: 5 June 2019

Published online: 28 June 2019

## References

1. Reddy, D. S. & Kutateladze, A. G. Structure revision of an acorane sesquiterpene cordycepol A. *Org. Lett.* **18**, 4860–4863 (2016).
2. Shi, Q. W., Sauriol, F., Lesimple, A. & Zamir, L. O. First three examples of taxane-derived di-propellanes in *taxus canadensis* needles. *Chem. Commun.* 544–545 (2004).
3. Tamber, U. K., Kano, T., Zepernick, J. F. & Stoltz, B. M. Convergent and diastereoselective synthesis of the polycyclic pyran core of saudin. *J. Org. Chem.* **71**, 8357–8364 (2006).
4. Yokoshima, S., Tokuyama, H. & Fukuyama, T. Enantioselective total synthesis of ( $\pm$ )-gelsemine: Determination of its absolute configuration. *Angew. Chem. Int. Ed.* **39**, 4073–4075 (2000).
5. Madin, A. et al. Use of the intramolecular heck reaction for forming congested quaternary carbon stereocenters. stereocontrolled total synthesis of ( $\pm$ )-gelsemine. *J. Am. Chem. Soc.* **127**, 18054–18065 (2005).
6. Vetica, F., Chauhan, P., Dochain, S. & Enders, D. Asymmetric organocatalytic methods for the synthesis of tetrahydropyrans and their application in total synthesis. *Chem. Soc. Rev.* **46**, 1661–1674 (2017).
7. Ye, N., Chen, H., Wold, E. A., Shi, P.-Y. & Zjou, J. Therapeutic potential of spirooxindoles as antiviral agents. *ACS Infect. Dis.* **2**, 382–392 (2016).
8. Cheng, D., Ishihara, Y., Tan, B. & Barbas, C. F. III Organocatalytic asymmetric assembly reactions: synthesis of spirooxindoles via organocascade strategies. *ACS Catal.* **4**, 743–762 (2014).
9. Zhang, L.-L., Zhang, J.-W., Xiang, S.-H., Guo, Z. & Tan, B. Remote control of axial chirality: synthesis of spirooxindole-urazoles via desymmetrization of ATAD. *Org. Lett.* **20**, 6022–6026 (2018).
10. Wang, L. et al. Switchable access to different spirocyclopentane oxindoles by N-heterocyclic carbene catalyzed reactions of isatin-derived enals and N-sulfonyl ketimines. *Angew. Chem. Int. Ed.* **56**, 8516–8521 (2017).
11. Chaudhari, P. D., Hong, B.-C. & Lee, G.-H. Organocatalytic enantioselective Michael–Michael–Michael–aldol condensation reactions: control of six stereocenters in a quadruple-cascade asymmetric synthesis of polysubstituted spirocyclic oxindoles. *Org. Lett.* **19**, 6112–6115 (2017).
12. Yoon, H., Rolz, M., Landau, F. & Lautens, M. Palladium-catalyzed spirocyclization through C–H activation and regioselective alkyne insertion. *Angew. Chem. Int. Ed.* **56**, 10920–10923 (2017).
13. Wu, H.-R. et al. FeCl<sub>3</sub>-mediated radical tandem reactions of 3-benzyl-2-oxindoles with styrene derivatives for the stereoselective synthesis of spirocyclohexene oxindoles. *Org. Lett.* **18**, 1382–1385 (2016).
14. Zhao, X. et al. The asymmetric synthesis of polycyclic 3-spirooxindole alkaloids via the cascade reaction of 2-isocyanooethylindoles. *Chem. Commun.* **51**, 16076–16079 (2015).
15. Jiang, K., Jia, Z.-J., Yin, X., Wu, L. & Chen, Y.-C. Asymmetric quadruple aminocatalytic domino reactions to fused carbocycles incorporating a spirooxindole motif. *Org. Lett.* **12**, 2766–2769 (2010).
16. Lu, Y.-L., Sun, J., Xie, Y.-J. & Yan, C.-G. Molecular diversity of the cyclization reaction of 3-methyleneoxindoles with 2-(3,4-dihydronaphthalen-1(2H)-ylidene)malononitriles. *RSC Adv.* **6**, 23390–23395 (2016).
17. Chintalapudi, V., Galvin, E. A., Greenaway, R. L. & Anderson, E. A. Combining cycloisomerization with trienamine catalysis: a regiochemically flexible enantio- and diastereoselective synthesis of hexahydroindoles. *Chem. Commun.* **52**, 693–696 (2016).
18. Tan, B., Candeias, N. R. & Barbas, C. F. III Construction of bispirooxindoles containing three quaternary stereocentres in a cascade using a single multifunctional organocatalyst. *Nat. Chem.* **3**, 473–477 (2011).
19. Chen, P. et al. Auto-tandem cooperative catalysis using phosphine/palladium: reaction of Morita–Baylis–Hillman carbonates and allylic alcohols. *Angew. Chem. Int. Ed.* **58**, 4036–4040 (2019).
20. Zhang, H. et al. Diversified cycloisomerization/Diels–Alder reactions of 1,6-enynes through bimetallic relay asymmetric catalysis. *Angew. Chem. Int. Ed.* **58**, 5381–5385 (2019).
21. Huang, J.-R., Sohail, M., Taniguchi, T., Monde, K. & Tanaka, F. Formal (4 + 1) cycloaddition and enantioselective Michael–Henry cascade reactions to synthesize spiro[4,5]decanes and spirooxindole polycycles. *Angew. Chem. Int. Ed.* **56**, 5853–5857 (2017).
22. Liu, Y.-L. et al. One-pot tandem approach to spirocyclic oxindoles featuring adjacent spiro-stereocenters. *Angew. Chem. Int. Ed.* **52**, 13735–13739 (2013).
23. Zhou, R. et al. Organocatalytic cascade reaction for the asymmetric synthesis of novel chroman-fused spirooxindoles that potently inhibit cancer cell proliferation. *Chem. Commun.* **51**, 13113–13116 (2015).
24. Mao, H. et al. Organocatalytic oxa/aza-Michael–Michael cascade strategy for the construction of spiro [chroman/tetrahydroquinoline-3,3'-oxindole] scaffolds. *Org. Lett.* **15**, 4062–4065 (2013).
25. Zhao, K. et al. Organocatalytic domino oxa-Michael/1,6-addition reactions: asymmetric synthesis of chromans bearing oxindole scaffolds. *Angew. Chem. Int. Ed.* **55**, 12104–12108 (2016).
26. Kalvacherla, B., Batthula, S., Balasubramanian, S. & Palakodety, R. K. Transition-metal-free cyclization of propargylic alcohols with aryl: synthesis of 3-benzofuranyl-2-oxindole and 3-spirooxindole benzofuran derivatives. *Org. Lett.* **20**, 3824–3828 (2018).

27. Yang, Z.-T., Zhao, J., Yang, W.-L. & Deng, W.-P. Enantioselective construction of CF<sub>3</sub>-containing spirooxindole  $\gamma$ -actones via organocatalytic asymmetric Michael/lactonization. *Org. Lett.* **21**, 1015–1020 (2019).
28. Zhu, L. et al. Enantioselective construction of spirocyclic oxindole derivatives with multiple stereocenters via an organocatalytic Michael/aldol/hemiacetalization cascade reaction. *Org. Lett.* **18**, 2387–2390 (2016).
29. Peng, J., Ran, G.-Y., Du, W. & Chen, Y.-C. Divergent cyclization reactions of Morita–Baylis–Hillman carbonates of 2-cyclohexenone and isatylidene malononitriles. *Org. Lett.* **17**, 4490–4493 (2015).
30. Zhao, S., Lin, J.-B., Zho, Y.-Y., Liang, Y.-M. & Xu, P.-F. Hydrogen-bond-directed formal [5 + 1] annulations of oxindoles with ester-linked bisenones: facile access to chiral spirooxindole  $\delta$ -lactones. *Org. Lett.* **16**, 1802–1805 (2014).
31. Du, D. et al. A novel diketopyrrolopyrrole (DPP)-based [2]rotaxane for highly selective optical sensing of fluoride. *Org. Lett.* **14**, 1274–1277 (2012).
32. Wang, J., Crane, E. A. & Scheidt, K. A. Highly stereoselective Brønsted acid catalyzed synthesis of spirooxindole pyrans. *Org. Lett.* **13**, 3086–3089 (2011).
33. Cui, H.-L. & Tanaka, F. Catalytic enantioselective formal hetero-Diels–Alder reactions of enones with isatins to give spirooxindole tetrahydropyranones. *Chem. Eur. J.* **19**, 6213–6216 (2013).
34. Peng, J.-B. et al. Efficient oxa-Diels–Alder/semipinacol rearrangement/aldol cascade reaction: short approach to polycyclic architectures. *Org. Lett.* **17**, 1014–1017 (2015).
35. Liu, G., Shirley, M. E., Van, K. N., McFarlin, R. L. & Romo, D. Rapid assembly of complex cyclopentanes employing chiral,  $\alpha,\beta$ -unsaturated acylammonium intermediates. *Nat. Chem.* **5**, 1049–1057 (2013).
36. Xu, K., Lalic, G., Sheehan, S. M. & Shair, M. D. Dynamic kinetic resolution during a cascade reaction on substrates with chiral all-carbon quaternary centers. *Angew. Chem. Int. Ed.* **44**, 2259–2261 (2005).
37. Bocknack, B. M., Wang, L.-C. & Krishe, M. J. Desymmetrization of enone-diones via rhodium-catalyzed diastereo- and enantioselective tandem conjugate addition-aldol cyclization. *Proc. Natl Acad. Sci.* **101**, 5421–5424 (2004).
38. Corbett, M. T. & Johnson, J. S. Dynamic kinetic asymmetric transformations of  $\beta$ -stereogenic  $\alpha$ -ketoesters by direct aldolization. *Angew. Chem. Int. Ed.* **53**, 255–259 (2014).
39. Zhang, H., Lin, S. & Jacobsen, E. N. Enantioselective selenocyclization via dynamic kinetic resolution of seleniranium ions by hydrogen-bond donor catalysts. *J. Am. Chem. Soc.* **136**, 16485–16488 (2014).
40. Chouthaiwale, P. V., Aher, R. D. & Tanaka, F. Catalytic enantioselective formal (4 + 2) cycloaddition by aldol-aldol annulation of pyruvate derivatives

with cyclohexane-1,3-diones to afford functionalized decalins. *Angew. Chem. Int. Ed.* **57**, 13298–13301 (2018).

## Acknowledgements

We thank Dr Michael Chandro Roy, Research Support Division, Okinawa Institute of Science and Technology Graduate University for mass analyses. This study was supported by the Okinawa Institute of Science and Technology Graduate University.

## Author contributions

M.S. and F.T. conceived the work, M.S. conducted the experiments, F.T. directed the research, M.S. and F.T. analyzed the data, and M.S. and F.T. wrote the manuscript.

## Additional information

**Supplementary information** accompanies this paper at <https://doi.org/10.1038/s42004-019-0177-5>.

**Competing interests:** The authors declare no competing interests.

**Reprints and permission** information is available online at <http://npg.nature.com/reprintsandpermissions/>

**Publisher's note:** Springer Nature remains neutral with regard to jurisdictional claims in published maps and institutional affiliations.



**Open Access** This article is licensed under a Creative Commons Attribution 4.0 International License, which permits use, sharing, adaptation, distribution and reproduction in any medium or format, as long as you give appropriate credit to the original author(s) and the source, provide a link to the Creative Commons license, and indicate if changes were made. The images or other third party material in this article are included in the article's Creative Commons license, unless indicated otherwise in a credit line to the material. If material is not included in the article's Creative Commons license and your intended use is not permitted by statutory regulation or exceeds the permitted use, you will need to obtain permission directly from the copyright holder. To view a copy of this license, visit <http://creativecommons.org/licenses/by/4.0/>.

© The Author(s) 2019